COMMUNICATION

Reversible Optical Writing and Data Storage in an Anthracene-Loaded Metal-Organic Framework

Min Tu,[a] Helge Reinsch,[b] Sabina Rodríguez-Hermida,[a] Rhea Verbeke,[a] Timothée Stassin,[a] Werner Egger,[c] Marcel Dickmann,[d] Bjorn Dieu,[e] Johan Hofkens,[e] Ivo Vankelecom,[a] Norbert Stock,[b] Rob Ameloot*[a]
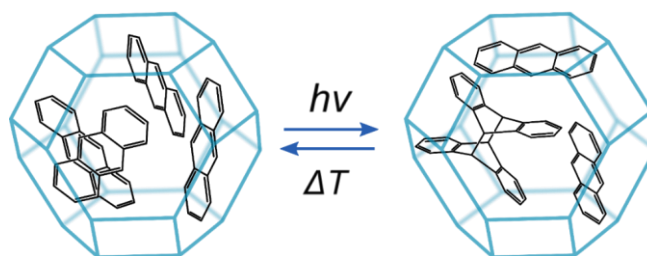
Abstract: Metal-organic frameworks (MOFs) enable the design of host-guest systems with specific properties. In this work, we show how confinement of anthracene in a well-chosen MOF host leads to reversible yellow-to-purple photoswitching of the fluorescence emission. This behavior has not been observed before for anthracene, either in pure form or adsorbed in other porous hosts. The photoresponse of the host-guest system is caused by the photodimerization of anthracene, which is greatly facilitated by the pore geometry, connectivity and volume as well as the structural flexibility of the MOF host. The photoswitching behavior is used to fabricate photopatternable and erasable surfaces that, in combination with data encryption and decryption, hold promise in product authentication and secure communication applications.

*T*ightly confined molecules behave differently from their free counterparts, through an interplay of adsorption, steric factors, and intermolecular forces. In nature, well-designed nanoenvironments (e.g., in enzymes) facilitate reactions by making use of shape-selective adsorption, energy transfer, restricted substrate motion, etc.[1–3] Synthetic materials can offer tailored nanoenvironments as well.[4–6] Metal-organic frameworks (MOFs) are crystalline solids that consist of inorganic nodes connected by multi-topic organic linkers.[7] The crystallinity, structural flexibility, tunable pore size and chemical functionalization of MOFs are ideal to capture and confine guest molecules in a variety of well-defined nanoenvironments.[8–12] The confinement of guest dye molecules in MOFs can induce photo-physical properties different from either component in isolation.[10] In addition, such dye molecules can respond to an external stimulus, thereby changing the adsorption, molecular transport or luminescence properties of the host-guest material.[13–16] Among different possible stimuli, light is a particularly attractive one with respect to applications.[14–16]

Luminescent materials that undergo reversible photoswitching are essential components for optoelectronic devices and optical data storage.[17,18] Although a variety of photoswitchable organic molecules has been developed, most switching phenomena occur exclusively in solution and are therefore challenging to integrate with solid-state optical devices.[19] As an example, the UV-induced photodimerization of anthracene (ANT) to a non-fluorescent photodimer is well-characterized and of special interest in photoswitching.[20,21] This photodimer can be dissociated either photochemically, by irradiation in the 250-290 nm range, or thermally at 250-340 °C.[20] However, the ANT photodimerization has so far only been reported in solution. One promising route towards leveraging the properties of photoswitchable molecules in the solid state is the confinement of light-responsive molecules as guests in a light-stable host material.[22] Although ANT confined in porous matrices such as zeolites and MOFs has previously been studied, no photoswitching has been reported to the best of our knowledge.[23–25]

In this work, we confined ANT in ZIF-8 (also known as MAF-4), a MOF material with a sodalite (SOD) topology formed by Zn(II) and 2-methlyimidazolate (mIm).[26,27] For the first time, reversible solid-state photoswitching of the ANT luminescence was observed, from yellow to purple emission (Scheme 1). Due to pairwise ordering in the ZIF-8 cage, the ANT guests initially show yellow excimer emission. Upon UV irradiation, half of the ANT molecules form a non-fluorescent photodimer, leaving the remaining guests randomly distributed in the cage and displaying purple monomer emission. This process is reversible as the excimer emission can be restored by thermal treatment and therefore enables photopatternable and erasable films with incorporated ANT@ZIF-8.

[a] Dr. M. Tu, Dr. S. Rodríguez-Hermida, R. Verbeke, T. Stassin, Prof. I. Vankelecom, Prof. R. Ameloot
Center for Surface Chemistry and Catalysis
KU Leuven-University of Leuven
Celestijnenlaan 200F, 3000 Leuven, Belgium
E-mail: rob.ameloot@kuleuven.be

[b] Dr. H. Reinsch, Prof. N. Stock
Institut für Anorganische Chemie
Christian-Albrechts-Universität Kiel
Christian-Albrechts-Platz 4, 24118 Kiel, Germany

[c] Dr. W. Egger
Institut für Angewandte Physik und Messtechnik LRT2
Universität der Bundeswehr München
Werner-Heisenberg-Weg 39, 85577 Neubiberg, Germany

[d] Dr. M. Dickmann
Heinz Maier-Leibnitz Zentrum (MLZ) and Physik Department E21
Technische Universität München
Lichtenbergstraße 1, 85748 Garching, Germany

[e] B. Dieu, Prof. J. Hofkens
Department of Molecular Visualization and Photonics
KU Leuven-University of Leuven
Celestijnenlaan 200F, 3000 Leuven, Belgium.

Supporting information for this article is given via a link at the end of the document.

Scheme 1. Proposed photoreaction in the ZIF-8 cage. 4 ANT molecules are ordered as 2 pairs in a twisted and partially overlapping geometry in the cage, giving rise to yellow excimer emission. After the irradiation under UV light, 2 ANT molecules from each of the pair photodimerize to form a non-fluorescent ANT photodimer. Because of steric hindrance, the other 2 ANT cannot photodimerize and lose the ordering, leading to purple monomer emission. The excimer emission can be restored through thermal dissociation of ANT photodimer and re-organization of ANT into ordered pairs.

ZIF-8 has spherical cavities of 11.6 Å in diameter interconnected by narrow windows of 3.4 Å in diameter.[27] Previously, encapsulation of guest molecules in ZIF-8 has been attempted during framework formation or post-synthetically by adsorption from a guest solution.[28,29] However, in both cases it is challenging to achieve high loadings due to solubility issues of the guest and the competition of solvent molecules. Therefore, ANT was loaded into ZIF-8 through post-synthetic sublimation. The success of this approach for ANT (5.6 × 9.8 Å²),[23] is likely enabled by flexibility of the host framework.[30–33] Powder X-ray diffraction (PXRD) after loading shows that the 2θ positions of all characteristic reflections remain unchanged, demonstrating the retention of long-range order (Figure 1a). The increase of the (200) and (211) reflection intensities are ascribed to electron density increases in the corresponding crystallographic planes due to the presence of ANT molecules.[34] The loss of N_2 adsorption capacity after ANT loading is another clear indication that the cages are occupied (Figure 1b). Solution ¹H NMR of acid-digested ANT@ZIF-8 reveals a maximum loading of 3.6 ANT guests per cage, corresponding to an ANT:mIm ratio of 0.3 (Figure S5). Thermal gravimetric analysis (TGA) reveals a 32 wt% guest loading (Figure 1d), corresponding to 3.6 ANT per cage (Supporting Information Section 1), in good agreement with the NMR data. These measurements reflect the average ANT occupancy; considering the possibility of a small amorphous or impurity fraction, each cage likely contains 4 ANT molecules.
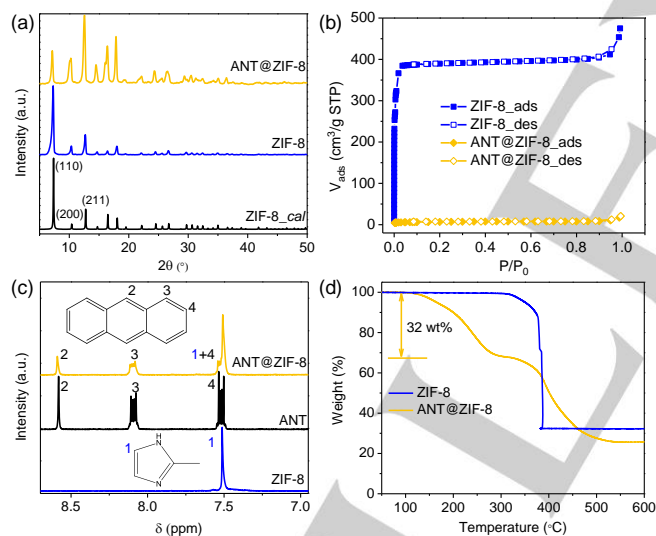

Figure 1. Characterization of ANT@ZIF-8. (a) PXRD patterns of ANT@ZIF-8, ZIF-8 and calculated ZIF-8. (b) N_2 sorption isotherms of ZIF-8 and ANT@ZIF-8 at 77 K. The BET surface areas of ZIF-8 and ANT@ZIF-8 are 1464 and 11 m²/g, respectively. (c) Solution ¹H NMR spectra of ANT (in DMSO-d₆) and acid-digested ZIF-8 and ANT@ZIF-8 (in DCI/D₂O/DMSO-d₆). (D) TGA of ZIF-8 and ANT@ZIF-8 under air.

The fluorescence of ANT@ZIF-8 shows a broad band (λ_{max} = 550 nm) that can be ascribed to ANT excimer emission (Figure 2a).[24,35] After UV irradiation (λ = 360 nm) for 30 min, several new bands (λ_{max} = 415 nm) appear, together with the disappearance of the 550 nm emission. These new bands are similar to the emission of a dilute ANT solution (1 mM in methanol), albeit slightly red-shifted, thus indicating the emergence of ANT monomers. Monitoring the fluorescence under continuous UV irradiation reveals the simultaneous enhancement of the monomer emission and decay of the excimer emission (Figure 2b). These kinetic data represent the overall photoresponse of powder packed in a 1 mm cuvette, thus corresponding to a relatively long path length for the UV light. The overall photoresponse is significantly faster when less material or a higher intensity UV light is used (Figure S13). The excimer emission can be fully recovered through heating (120 °C, 2 days). Since this reversible excimer-to-monomer photoswitching has not been reported for ANT in any other porous host, it seems that the ZIF-8 host plays a crucial role.
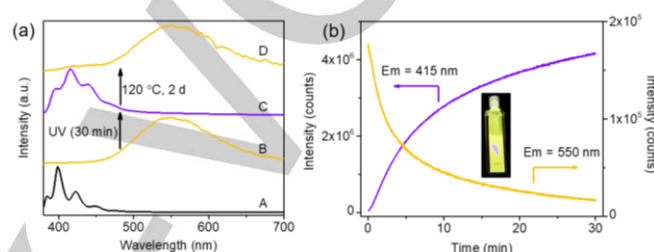

Figure 2. Photoswitching of ANT@ZIF-8. (a) Fluorescence emission spectra of 1 mM ANT methanol solution (A), ANT@ZIF-8 (B), UV-irradiated ANT@ZIF-8 (C) and thermally treated UV-irradiated ANT@ZIF-8 (D). (b) In situ monitoring of the fluorescence emission intensity (415 nm and 550 nm) upon continuous excitation at λ = 360 nm. Inset: Image of a cuvette containing ANT@ZIF-8 powder under a 366 nm UV lamp after irradiation (λ = 360 nm, 30 min) in the fluorimeter. The purple spot indicates the photoswitching.

To study the chemistry behind the photoswitching, several characterization techniques were combined. First, the structure of ANT@ZIF-8 was determined by PXRD and Rietveld refinement (Supporting Information Section 2). After ANT encapsulation, the cubic ZIF-8 structure (*I*-43m) turns to monoclinic (*C*2) with altered Zn-Zn distances (Figure S3). Symmetry changes by guest loading are commonly observed in MOFs,[36] but have not been reported for ZIF-8 (Table S3). In previous studies, only mIm linker rotation has been observed during guest adsorption, followed by relaxation and a return to the initial conformation.[30] The linker rotation was also observed when applying high pressure to ZIF-8 in hydrostatic medium, but the *I*-43m symmetry was still maintained.[32,33] Nevertheless, the crystalline nature of ANT@ZIF-8 allows to determine that the 4 guest molecules in the cage are ordered as 2 pairs, in a twisted and partially overlapping geometry (Figure 3a-b). This geometry of the ANT pair allows sufficient π-orbital overlap for ANT excimer formation. We hypothesize that UV light induces the photodimerization of the 2 ANT molecules closest to the center of the cage, one from each pair, to form a non-fluorescent photodimer, and the remaining 2 ANT molecules are randomly distributed in the cage, resulting in monomer emission (Scheme 1). In accordance with this hypothesis, solution ¹H NMR measurements of acid-digested ANT@ZIF-8 show the formation of ANT photodimer upon UV irradiation by the signal at δ = 4-7 ppm (Figure 3c). Importantly, the molar ratio of ANT monomer to photodimer is determined to be 2:0.9, which is very close to the ratio of 2:1 expected for the

proposed scenario. This also confirms the proposed loading of 4 ANT per cage. If many cages would contain 3 molecules, monomer emission would be observed already before UV irradiation. After thermal treatment of the irradiated ANT@ZIF-8, the ^{1}H NMR signal at δ = 4-7 ppm disappears (Figure 3c), demonstrating the dissociation of the photodimer. Because of its reduced conjugation, the photodimer does not absorb light at wavelengths > 300 nm and UV-Vis spectroscopy can be used to monitor the photodimerization within ANT@ZIF-8 (Figure 3d).[37] In accordance with the hypothesis above, the absorption of ANT@ZIF-8 rapidly decreases upon UV irradiation to reach a constant value after 30 min. In addition, after UV irradiation, the distorted ZIF-8 structure returns to its initial cubic symmetry together with a non-ordered arrangement of guest molecules (Figure S4 and Table S4).
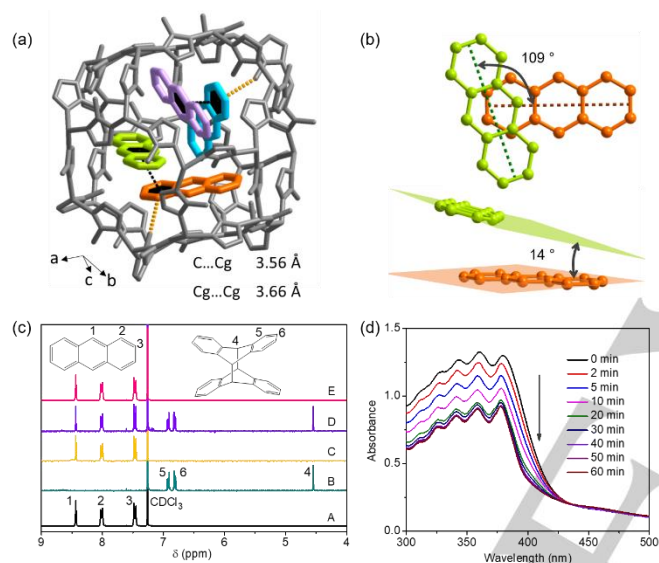

Figure 3. Characterization of the photoswitching of ANT@ZIF-8. (a) Crystal structure of ANT@ZIF-8 obtained by Rietveld refinement: the atoms (Zn, C and N) of ZIF-8 are shown in grey and H atom is not modeled, and ANT molecules in the cage are illustrated in other colors (orange, green, violet and cyan). The yellow dash lines highlight the closest distance (3.56 Å) between ANT centroid rings (orange and cyan) and C atoms from the methyl groups of mIm linker. The exact position of H atoms in the methyl group is not modeled. However, considering the close distance of C and ANT centroid ring, it is proposed that there is a C-H···π interaction that stabilizes the two ANT molecules in the cage. 2 ANT rings are inclined toward each other with a π···π distance of 3.66 Å, indicating the presence of strong π···π interaction. (b) Top (top) and side (bottom) view of one of the ANT pairs in the cage. When viewed from the top, the 2 ANT aromatic planes are almost perpendicular at angle of 109 °. When viewed from the side, the 2 ANT rings are inclined toward each other at an angle of 14 °. (c) Solution ^{1}H NMR spectra of ANT (A), ANT photodimer (B), ANT@ZIF-8 (C), UV-irradiated (λ = 350 nm, 2 h) ANT@ZIF-8 (D) and thermally (120 °C, 2 days) treated UV-irradiated ANT@ZIF-8 (E). ANT and ANT photodimer were dissolved in CDCl$_3$ and the other powder samples were dissolved in DCl/D$_2$O/CDCl$_3$. (d) UV-Vis absorption spectra of ANT@ZIF-8 irradiated with 366 nm UV light for different times.

Interestingly, photoswitching was also observed for ANT@ZIF-8 with loadings lower than 3.6 ANT per cage (Figure S21). Even at very low loading (0.24 ANT per cage), excimer emission is observed, next to the expected monomer emission.

Once the loading reaches 1 ANT per cage, the excimer emission band dominates the emission spectrum. Moreover, the UV-induced enhancement of the monomer fluorescence intensity is observed for all loadings. In addition, the remaining free space after ANT loading was studied by positron annihilation lifetime spectroscopy (PALS) together with N$_2$ sorption. PALS is a technique to quantify the size of free-volume elements in porous materials.[38] With increasing ANT loading, the free volume present in the cage decreases (Figure S23), in agreement with the N$_2$ sorption data (Figure S22). The typical ZIF-8 lifetime is detected for loadings up to 1.44 ANT per cage, suggesting the presence of empty cages at lower loadings. Furthermore, at full loading, PALS confirms the absence of empty cages. These results suggest that (i) when loaded into ZIF-8, ANT molecules prefer to sit in pairs instead of as monomers, even at overall loadings much lower than 2 per cage; (ii) the configuration of 2 pairs per cage is preferred over having single pairs in separate cages, as indicated by the UV-induced enhancement of monomer emission.

The well-defined ZIF-8 pores contribute in several ways to the photoswitching behavior of the host-guest system. First, the pore size together with the structural flexibility allows the preferential encapsulation of 4 ANT per cage. If the loading amount would be less or more than 4 ANT per cage, photoswitching may not happen or be less pronounced. Second, because of the confinement, ANT favors a well-ordered configuration that results in excimer emission. Third, the sufficiently large cage facilitates the photodimerization of 2 ANT molecules, but prevents complete reaction of all guests and therefore avoids complete fluorescence quenching. Fourth, because of trapping in the SOD cage, the thermally dissociated ANT pairs rearrange and again adopt the initial well-ordered geometry, thereby enabling reversible photoswitching.

Photoswitching materials have potential for product authentication.[39-41] To explore this avenue, proof-of-concept photopatternable paper was fabricated by drop-casting a ANT@ZIF-8 suspension in methanol on filter paper. Photopatterning was performed by UV irradiation of the paper through a simple polyester photomask (Figure 4a). Both positive and negative images were achieved with a resolution better than 1 mm, which could be readily improved using better masks (Figure 4a). Importantly, the patterns are invisible under ambient light and can only be read by UV light (Figure S24). Such photopatternable paper can be employed to develop hidden labels with important information (e.g., serial number or website) encoded in quick response (QR) codes (Figure 4b). In addition, the same UV wavelength can be used for writing information into the ANT@ZIF-8 composite as well as reading it out and subsequently erasing the pattern (Figure 4b). Thus, write-once-read-once authentication tokens can be developed by optimizing the intensity of the read-out light and the quantity of the photoswitching material. The reversibility of the switching behavior upon thermal treatment enables 'resetting' and reuse (Supporting Information Section 8). Besides product authentication, this technique may enable the secure delivery of information, because the data can be erased during readout and cannot be regenerated.
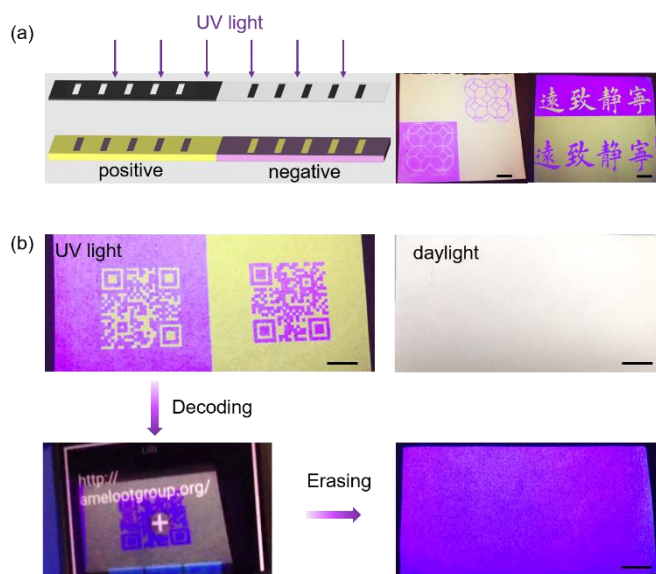
Figure 4. Photopatterning on ANT@ZIF-8 based paper. (a) Schematic representation of photopatterning on ANT@ZIF-8 based paper in combination of positive and negative ways (left) and optical images obtained by photopatterning (right, scale bar: 2 cm). (b) Top: images of photopatterned QR codes under UV light and day light. Bottom: decoding of QR codes by a smartphone (left) and erasing the codes after encoding (right). Scale bar: 1 cm.

In conclusion, solid-state reversible photoswitching was observed for photoreactive ANT guests confined within the cages of ZIF-8. 4 well-organized ANT molecules were encapsulated, giving rise to excimer emission. The limited space in the cage only permits 2 ANT molecules to photodimerize, resulting in 1 non-fluorescent ANT photodimer and 2 randomly distributed ANT molecules that emit as monomers. Thermal dissociation of the ANT photodimer switches the system back to its initial excimer emission. This phenomenon relies on the unique properties of ZIF-8, i.e., pore geometry, long-range ordering, structural flexibility and suitable pore volume. The solid-state photoswitching allowed the development of photopatternable, erasable and rewritable paper with potential applications in production authentication and secure communication. We believe that MOF-based host-guest chemistry promises further interesting phenomena, building on other photochemical transformations (e.g., trans-cis isomerization, ionization, pericyclic ring-opening and ring-closing). Supported by ongoing efforts to integrate MOFs in devices,[42] these phenomena may be exploited in opto-electronics.

Acknowledgements

[1] T. S. Koblenz, J. Wassenaar, J. N. H. Reek, *Chem. Soc. Rev.* **2008**, *37*, 247-262.
[2] S. Zarra, D. M. Wood, D. A. Roberts, J. R. Nitschke, *Chem. Soc. Rev.* **2015**, *44*, 419-432.
[3] D. Ajami, J. Rebek, *Acc. Chem. Res.* **2013**, *46*, 990-999.
[4] B. M. Weckhuysen, J. Yu, *Chem. Soc. Rev.* **2015**, *44*, 7022-7024.
[5] S. Das, P. Heasman, T. Ben, S. Qiu, *Chem. Rev.* **2017**, *117*, 1515-1563.
[6] X.-Y. Yang, L.-H. Chen, Y. Li, J. Claire Rooke, C. Sanchez, B.-L. Su, *Chem. Soc. Rev.* **2017**, *46*, 481-558.
[7] S. R. Batten, N. R. Champness, X.-M. Chen, J. Garcia-Martinez, S. Kitagawa, L. Öhrström, M. O'Keeffe, M. Paik Suh, J. Reedijk, *Pure Appl. Chem.* **2013**, *85*, 1715-1724.
[8] S. Kitagawa, R. Kitaura, S. Noro, *Angew. Chem. Int. Ed.* **2004**, *43*, 2334-2375.
[9] H. Furukawa, K. E. Cordova, M. O'Keeffe, O. M. Yaghi, *Science* **2013**, *341*, 1230444.
[10] M. D. Allendorf, M. E. Foster, F. Léonard, V. Stavila, P. L. Feng, F. P. Doty, K. Leong, E. Y. Ma, S. R. Johnston, A. A. Talin, *J. Phys. Chem. Lett.* **2015**, *6*, 1182-1195.
[11] T. H. Noh, O.-S. Jung, *Acc. Chem. Res.* **2016**, *49*, 1835-1843.
[12] U. Ryu, H. S. Lee, K. Park, K. M. Choi, *Polyhedron* **2018**, *154*, 275-294.
[13] N. Yanai, K. Kitayama, Y. Hijikata, H. Sato, R. Matsuda, Y. Kubota, M. Takata, M. Mizuno, T. Uemura, S. Kitagawa, *Nat. Mater.* **2011**, *10*, 787-793.
[14] N. Yanai, T. Uemura, M. Inoue, R. Matsuda, T. Fukushima, M. Tsujimoto, S. Isoda, S. Kitagawa, *J. Am. Chem. Soc.* **2012**, *134*, 4501-4504.
[15] J. Yu, Y. Cui, C.-D. Wu, Y. Yang, B. Chen, G. Qian, *J. Am. Chem. Soc.* **2015**, *137*, 4026-4029.
[16] H. A. Schwartz, U. Ruschewitz, L. Heinke, *Photochem. Photobiol. Sci.* **2018**, *17*, 864-873.
[17] S. Kawata, Y. Kawata, *Chem. Rev.* **2000**, *100*, 1777-1788.
[18] J. M. Baumes, J. J. Gassensmith, J. Giblin, J.-J. Lee, A. G. White, W. J. Culligan, W. M. Leevy, M. Kuno, B. D. Smith, *Nat. Chem.* **2010**, *2*, 1025-1030.
[19] W. R. Browne, B. L. Feringa, *Annu. Rev. Phys. Chem.* **2009**, *60*, 407-428.
[20] H. Bouas-Laurent, A. Castellan, J.-P. Desvergne, R. Lapouyade, *Chem. Soc. Rev.* **2000**, *29*, 43-55.
[21] H. Bouas-Laurent, A. Castellan, J.-P. Desvergne, R. Lapouyade, *Chem. Soc. Rev.* **2001**, *30*, 248-263.
[22] B. Gui, Y. Meng, Y. Xie, K. Du, A. C.-H. Sue, C. Wang, *Macromol. Rapid Commun.* **2018**, *39*, 1700388.
[23] F. Márquez, H. García, E. Palomares, L. Fernández, A. Corma, *J. Am. Chem. Soc.* **2000**, *122*, 6520-6521.
[24] O.-H. Kwon, H. Yu, D.-J. Jang, J. Phys. Chem. B 2004, 108, 3970-3974.
[25] T. Kitao, R. Hongu, S. Kitagawa, T. Uemura, *Chem. Lett.* **2017**, *46*, 1705-1707.
[26] K. S. Park, Z. Ni, A. P. Côté, J. Y. Choi, R. Huang, F. J. Uribe-Romo, H. K. Chae, M. O'Keeffe, O. M. Yaghi, *Proc. Natl. Acad. Sci.* **2006**, *103*, 10186-10191.
[27] X.-C. Huang, Y.-Y. Lin, J.-P. Zhang, X.-M. Chen, *Angew. Chem. Int. Ed.* **2006**, *45*, 1557-1559.
[28] N. Liédana, A. Galve, C. Rubio, C. Téllez, J. Coronas, *ACS Appl. Mater. Interfaces* **2012**, *4*, 5016-5021.

[29] I. B. Vasconcelos, T. G. da Silva, G. C. G. Militão, T. A. Soares, N. M. Rodrigues, M. O. Rodrigues, N. B. da Costa, R. O. Freire, S. A. Junior, *RSC Adv.* **2012**, *2*, 9437-9442.

[30] D. Peralta, G. Chaplais, J.-L. Paillaud, A. Simon-Masseron, K. Barthelet, G. D. Pirngruber, *Microporous Mesoporous Mater.* **2013**, *173*, 1-5.

[31] D. I. Kolokolov, A. G. Stepanov, H. Jobic, *J. Phys. Chem. C* **2015**, *119*, 27512-27520.

[32] S. A. Moggach, T. D. Bennett, A. K. Cheetham, *Angew. Chem. Int. Ed.* **2009**, *48*, 7087-7089.

[33] J. Im, N. Yim, J. Kim, T. Vogt, Y. Lee, *J. Am. Chem. Soc.* **2016**, *138*, 11477-11480.

[34] D. Esken, H. Noei, Y. Wang, C. Wiktor, S. Turner, G. V. Tendeloo, R. A. Fischer, *J. Mater. Chem.* **2011**, *21*, 5907-5915.

[35] T. Hinoue, Y. Shigenoi, M. Sugino, Y. Mizobe, I. Hisaki, M. Miyata, N. Tohnai, *Chem. – Eur. J.* **2012**, *18*, 4634-4643.

[36] A. Schneemann, V. Bon, I. Schwedler, I. Senkovska, S. Kaskel, R. A. Fischer, *Chem. Soc. Rev.* **2014**, *43*, 6062-6096.

[37] G. W. Breton, X. Vang, *J. Chem. Educ.* **1998**, *75*, 81-82.

[38] S. J. Tao, *J. Chem. Phys.* **1972**, *56*, 5499-5510.

[39] B. Yoon, J. Lee, I. S. Park, S. Jeon, J. Lee, J.-M. Kim, *J. Mater. Chem. C* **2013**, *1*, 2388-2403.

[40] C. Zhang, B. Wang, W. Li, S. Huang, L. Kong, Z. Li, L. Li, *Nat. Commun.* **2017**, *8*, 1138.

[41] H. Sun, S. Liu, W. Lin, K. Y. Zhang, W. Lv, X. Huang, F. Huo, H. Yang, G. Jenkins, Q. Zhao, et al., *Nat. Commun.* **2014**, *5*, 1.

[42] I. Stassen, N. Burtch, A. Talin, P. Falcaro, M. Allendorf, R. Ameloot, *Chem. Soc. Rev.* **2017**, *46*, 3185-3241.

Entry for the Table of Contents

COMMUNICATION

Confinement of anthracene molecules in a metal-organic framework enables reversible yellow-to-purple photoswitching of the fluorescence emission. The photoresponse of the host-guest system strongly relies on the unique properties of the MOF host, i.e., the pore geometry, connectivity and volume as well as the structural flexibility. The solid-state photoswitching allows the development of photopatternable, erasable and rewritable paper.

Photopatternable MOF
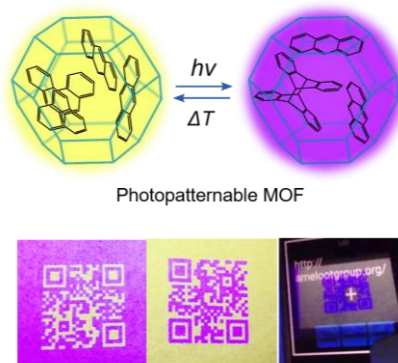
Min Tu, Helge Reinsch, Sabina Rodríguez-Hermida, Rhea Verbeke, Timothée Stassin, Werner Egger, Marcel Dickmann, Bjorn Dieu, Johan Hofkens, Ivo Vankelecom, Norbert Stock, Rob Ameloot*

Page No. – Page No.

Reversible Optical Writing and Data Storage in an Anthracene-Loaded Metal-Organic Framework